

RSC Advances



This is an *Accepted Manuscript*, which has been through the Royal Society of Chemistry peer review process and has been accepted for publication.

Accepted Manuscripts are published online shortly after acceptance, before technical editing, formatting and proof reading. Using this free service, authors can make their results available to the community, in citable form, before we publish the edited article. This *Accepted Manuscript* will be replaced by the edited, formatted and paginated article as soon as this is available.

You can find more information about *Accepted Manuscripts* in the [Information for Authors](#).

Please note that technical editing may introduce minor changes to the text and/or graphics, which may alter content. The journal's standard [Terms & Conditions](#) and the [Ethical guidelines](#) still apply. In no event shall the Royal Society of Chemistry be held responsible for any errors or omissions in this *Accepted Manuscript* or any consequences arising from the use of any information it contains.

Full Alignment of Dispersed Colloidal Nanorods by Alternating Electric Fields

Received 00th January 20xx,
Accepted 00th January 20xx

M. Mohammadimasoudi,^{a,c} Z. Hens^{b,c} and K. Neyts^{a,c}

DOI: 10.1039/x0xx00000x

www.rsc.org/

The parallel alignment of an ensemble of colloidal quantum rods may unleash their application as the optically anisotropic constituent in polarized fluorescent sheets or polarization-selective detectors. Here, we demonstrate that full alignment of colloidal CdSe/CdS nanorods in suspension can be achieved by applying AC electric fields. Alignment is monitored by the concurrent change of the optical transmission of the dispersion. By comparing the transmission measurements to a theoretical model encompassing both the permanent and induced dipole moments of the nanorods, we can attribute the alignment to the interaction between the electric field and the nanorod's permanent dipole moment. The permanent dipole moment, relaxation time, absorption anisotropy and critical frequency of the CdSe/CdS nanorods are determined. In addition, we show that the regime of full alignment enables the direct determination of the anisotropic absorption of CdSe/CdS nanorods. We find that the anisotropy in absorption for the CdSe dot is similar to that of the CdS rod, which we attribute to the similarity in dielectric constant and electric field in both materials.

Introduction

Over the last 30 years, colloidal nanocrystals have attracted wide scientific and technological interest since their optoelectronic properties can be tuned by means of their size and shape. Whereas size is the key parameter underlying quantization in semiconductor nanocrystals¹ and the occurrence of localized surface plasmon resonances in metal nanocrystals,² shape often adds unique possibilities to further adjust nanocrystal properties.³ In this respect, rods and platelets stand out since their shape anisotropy results in an anisotropic interaction – absorption, emission or scattering – with light.⁴ Metallic nanorods, for example, exhibit a splitting of the localized surface plasmon resonance into a longitudinal and transversal mode that most strongly interacts with light polarized perpendicular or parallel to the long axis of the rod, respectively.² Rod-like colloidal semiconductor nanocrystals such as CdSe quantum rods or CdSe/CdS dot-in-rods on the other hand more strongly absorb and emit light polarized parallel to their long axis.^{5,6}

Although use can be made of the anisotropic properties of single nanorods,^{2, 7, 8} applications such as polarized light emitting diodes,⁹ photovoltaic energy conversion, optical sensors or switches¹⁰⁻¹³ require layers or volumes with large ensembles of aligned nanorods. In this context, various methods for the collective alignment of colloidal nanorods have been explored. Focusing on colloidal quantum rods, these either exploit the tendency of nanorods to self-assemble by aligning their long axes upon drying or dispersion destabilization or involve the use of external forces to impose rod alignment. Depending on the actual conditions, slow

solvent evaporation on a solid substrate or a liquid subphase results in nanorod films aligned with their long axis parallel or perpendicular to the substrates.¹⁴⁻¹⁹ Alternatively, alignment by external forces has been demonstrated using mechanical rubbing of a pre-deposited film of randomly oriented quantum rods²⁰ or by means of electric fields applied either during solvent drying²¹⁻²³ or to achieve electrophoretic deposition.²⁴ Besides the alignment of nanorods during deposition, a number of studies have addressed the alignment of quantum rods in solution. Various reports describe the organization of nanorods in two-dimensional sheets of a single layer of parallel quantum rods by depletion attraction,²⁵ specific surface functionalization schemes²⁶ or a reduction of the dispersion stability.^{27, 28} Although it proved possible to orient such 2D sheets in solution by magnetic fields,²⁹ the size of the sheets leads to considerable scattering of light and results in patchy deposits upon solvent drying. Opposite from this alignment-by-aggregation, the collective orientation or alignment of non-aggregated nanorods is possible by means of an electric field. Although electrical alignment has mainly been used to characterize nanorod properties such as the dipole moment³⁰ or the absorption anisotropy,³¹ it can be regarded as a technical solution to produce functional solid films with strong anisotropy in optical absorption, emission or scattering. For example, alignment-in-solution can be achieved in a polymerizable medium, where a triggered polymerization can lock the rod orientation to produce self-supporting films or sheets of aligned nanorods. Such an approach can have several advantages. Depending on the electrode configuration, the alignment can be homogenous or follow a pattern. Moreover, in-solution alignment by an electric field is also possible at low nanorod concentrations, thus leading to films with a desired absorption coefficient for, e.g., optical down-conversion applications in lighting, displays or luminescent solar concentrators.

Despite the potential of in-solution alignment of nanorods by electric fields, both theoretical and experimental aspects have only been partially studied in the literature. Ruda et al. gave a theoretical description of the alignment of gold nanorods based on the anisotropy of the induced dipole moment.³² In

^a Electronics and Information Systems Department, Ghent University, St. Pietersnieuwstraat 41, 9000 Gent, Belgium.

^b Physics and Chemistry of Nanostructures, Ghent University, Krijgslaan 281-53, 9000 Gent, Belgium.

^c Center for Nano- and Biophotonics, Ghent University, Belgium.

Electronic Supplementary Information (ESI) available: Synthesis of CdSe/CdS nanorods; Photograph and transmission measurement of CdSe/CdS NR suspension in dodecane; Characteristic information and obtained data on CdSe/CdS NRs; Rotational relaxation frequency; Polarization ratio]. See DOI: 10.1039/x0xx00000x

the case of semiconductor nanorods on the other hand, the alignment by alternating electric fields is typically attributed to a permanent dipole along their long axis,^{21, 30, 31} although the presence of a permanent dipole could not be confirmed by electrostatic force microscopy.³³ In addition, there are no reports about reaching the regime of full nanorod alignment in the literature. Using the available combination of applied fields and quantum rod dipoles, Kamal et al. only obtained partial orientation, as the electrostatic energy gained by orienting the rods was at best about equal to the thermal energy,³¹ while an even weaker orientation can be deduced from the figures provided by Li et al.³⁰

In this paper, we demonstrate that colloidal CdSe/CdS nanorods that are dispersed in a non-polar solvent can be quasi fully aligned by applying sufficiently strong alternating electric fields. The degree of alignment is monitored by measuring the transmission³¹ as a function of time during the application of a time-dependent voltage. The measurement results are interpreted by using a dynamic model that encompasses the viscous drag of the solvent, the rotational diffusion of the nanorods, the torque due to the permanent dipole moment and the (induced) dielectric torque. The transition from random to full alignment as a function of the electric field enables us to attribute the alignment to the nanorods' permanent dipole and determine the dipole's magnitude. In addition, we show that full alignment and relaxation are established with characteristic time constants of 50 μ s or less. Finally, we demonstrate that the regime of full alignment is ideal to quantify the absorption anisotropy of colloidal NRs, where we find that the small dielectric mismatch between the CdS rod and the CdSe dot makes that CdSe-dot and CdS-rod related optical transitions feature a similar absorption anisotropy.

Experimental

CdSe/CdS nanorod synthesis

CdSe/CdS dot-in-rods are synthesized according to a procedure described in the literature (see Supporting Information S1 for synthesis details).²³ In brief, CdSe quantum dots (QDs) with a wurtzite structure and an average diameter of 2.3 nm are synthesized first. On these core QDs, an anisotropic CdS shell is grown using phosphonic acids as the ligands to obtain CdSe/CdS dot-in-rods, which we will denote as CdSe/CdS nanorods (NRs). Figure 1 provides an overview of the most important characteristics of the NRs used in this study. Based on the transmission electron micrograph (Figure 1a), their average diameter and length are estimated at 4.8 and 51.5 nm, respectively. Moreover, their absorbance spectrum (Figure 1b) indicates that they have a first exciton or band-gap transition at 560 nm, whereas the absorbance by the CdS rod starts dominating at wavelengths below 500 nm.

Quantum rod alignment by electric fields.

As shown in Figure 2a, a cell is made by joining two glass substrates with 1 cm² ITO electrodes with glue containing 20

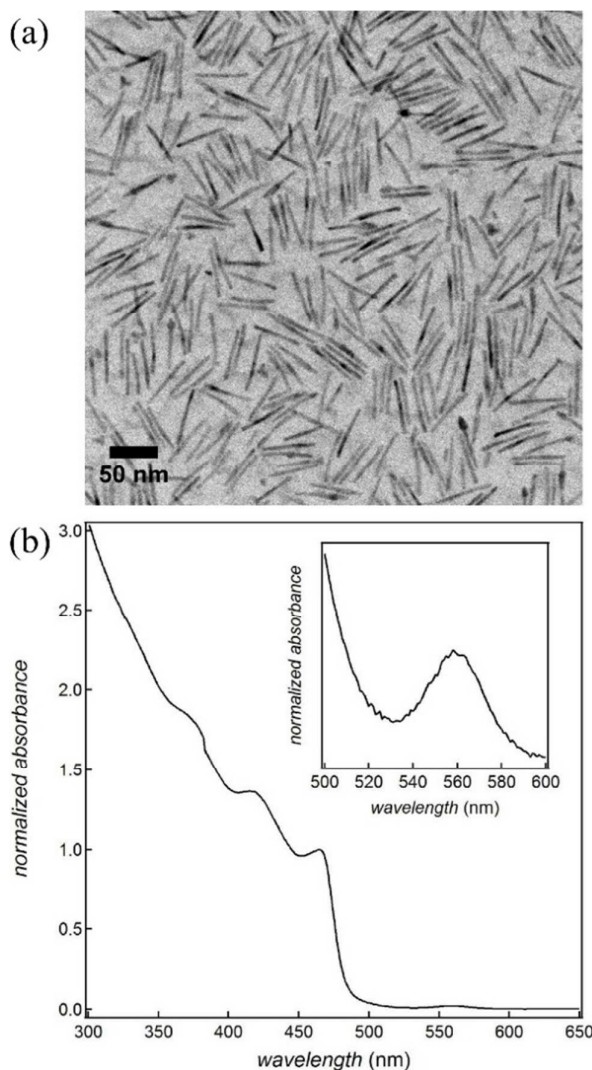


Figure 1. (a) TEM micrograph of the CdSe/CdS nanorods (b) Absorption spectrum of the CdSe/CdS nano rod dispersion, normalized at the first CdS absorption feature at ≈ 470 nm (inset: magnification on the range 500 to 600 nm highlighting the absorption feature of the CdSe cores).

or 50 μ m spacer beads (Sekisui Chemicals) to ensure a uniform cell gap d between the electrodes.

The cell is filled with the CdSe/CdS NR suspension by capillary force (see Supporting Information S2). A function generator (TTi-TG315) and a voltage amplifier are used to apply a high AC voltage V with a frequency between 50 Hz and 40 kHz over the cell. This results in electric fields – estimated as $E = V/d$ – of up to 40 V/ μ m in the dispersion. The transmission of blue (470 nm) and green (560 nm) LED light is measured using a photodetector (FLC electronics-PIN20) mounted on a microscope (Nikon-eclipse E400). Figure 2b shows part of the setup including the cell and the blue LED.

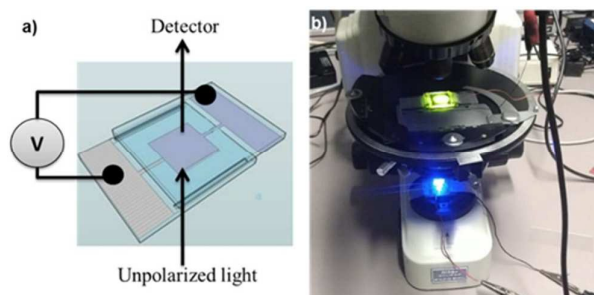


Figure 2. a) Schematic view of the cell used to align dispersed nanorods by means of electric fields and (b) image of the microscope transmission setup.

Theoretical Background

Orientation of spheroids in an electric field

As sketched in Figure 3a, the application of a voltage difference across the cell, and thus an electric field inside the dispersion, will change the random orientation of the long axis of the NRs into a preferential alignment along the electric field. To describe this electric-field driven alignment of NRs dispersed in an apolar liquid, we consider both their permanent and induced (dielectric) dipole moments. Whereas CdSe/CdS NRs have a permanent dipole moment that is related to their non-centro-symmetric wurtzite crystal structure, the induced dipole moment cannot be neglected *a priori* since semiconductor NRs typically have a considerably higher dielectric constant than the surrounding apolar liquid. To assess the characteristic times determining the motion of NRs under the action of an alternating field, we use a dynamic equation that takes into account both the dielectric and dipolar torques, thermal fluctuations and rotational viscosity of the NRs. When a NR – approximated as a prolate ellipsoid of revolution – is placed in a host medium with dielectric constant ϵ_h in which a homogeneous external field E is present, the induced dipole moment \mathbf{p}_{ind} with respect to the host medium amounts to:

$$\mathbf{p}_{ind} = \alpha_{\parallel} \epsilon_0 E_{\parallel} \mathbf{1}_{\parallel} + \alpha_{\perp} \epsilon_0 E_{\perp} \mathbf{1}_{\perp} \quad (1)$$

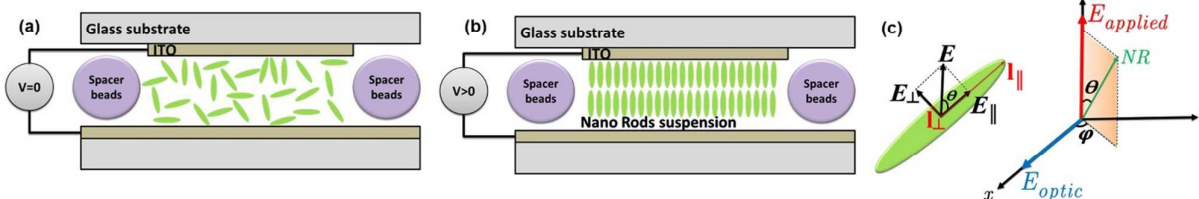


Figure 3. Orientation of NRs in suspension in dodecane (a) without and (b) with applied voltage. (c) The electric field is perpendicular to the ITO electrodes and θ is the angle between the applied electric field and the NR long axis. The components of the applied electric field parallel and perpendicular to the long axis $\mathbf{1}_{\parallel}$ are called E_{\parallel} and E_{\perp} respectively.

Here, the unit vectors $\mathbf{1}_{\parallel}$ and $\mathbf{1}_{\perp}$ are mutually orthogonal, pointing along and perpendicularly to the long axis of the ellipsoid, respectively (see Figure 3c). The field components E_{\parallel} and E_{\perp} are the respective projections of the electric field on $\mathbf{1}_{\parallel}$ and $\mathbf{1}_{\perp}$. For an anisotropic ellipsoid of revolution with dielectric constants ϵ_{\parallel} and ϵ_{\perp} , the concomitant polarizabilities α_{\parallel} and α_{\perp} are given by:³⁴

$$\alpha_{\parallel} = \frac{\epsilon_{\parallel} - \epsilon_h}{\epsilon_h + L_{\parallel}(\epsilon_{\parallel} - \epsilon_h)} V \quad (2)$$

$$\alpha_{\perp} = \frac{\epsilon_{\perp} - \epsilon_h}{\epsilon_h + L_{\perp}(\epsilon_{\perp} - \epsilon_h)} V$$

In the above expression, V represents the volume of a NR and L_{\parallel} and L_{\perp} are the depolarization factors for fields parallel and perpendicular to the NR long axis, respectively. With a and b the length of the corresponding semi-axes of the ellipsoid (see Figure 3c), these read:³⁵

$$L_{\parallel} = \frac{b^2}{a^2 - b^2} \left[\frac{a}{2\sqrt{a^2 - b^2}} \ln \frac{a + \sqrt{a^2 - b^2}}{a - \sqrt{a^2 - b^2}} - 1 \right] \quad (3)$$

$$L_{\perp} = \frac{1 - L_{\parallel}}{2}$$

The induced dipole moment leads to a dielectric or induced torque on the NR given by:

$$\mathbf{T}_{ind} = \mathbf{p}_{ind} \times \mathbf{E} = \frac{1}{2} (\alpha_{\parallel} - \alpha_{\perp}) \sin 2\theta \epsilon_0 E^2 \mathbf{1}'_{\perp} \quad (4)$$

Here, θ is the angle between the long axis of the ellipsoid and the electric field, whereas $\mathbf{1}'_{\perp}$ is the unit vector perpendicular to both $\mathbf{1}_{\parallel}$ and $\mathbf{1}_{\perp}$ (see Figure 3(c)).

If the NR has a permanent dipole moment \mathbf{p} along the long axis of the NR, then the external electric field leads to an additional dipolar torque \mathbf{T}_{dip} :

$$\mathbf{T}_{dip} = \mathbf{p} \times \mathbf{E} = pE \cos \theta \mathbf{1}'_{\perp} \quad (5)$$

Including the two torques into the dynamic equation of reorientation yields the following differential equation for the orientation angle θ :

$$I \frac{d^2\theta}{dt^2} + \gamma_r \frac{d\theta}{dt} = \sqrt{k_B T \gamma_r} \delta(t) + pE \cos \theta + \frac{1}{2}(\alpha_{\parallel} - \alpha_{\perp}) \sin 2\theta \varepsilon_0 E^2 \mathbf{1}'_{\perp} \quad (6)$$

The first term of eq 6 contains the moment of inertia I and is usually negligible for small ellipsoids, except at very high frequencies (*i.e.*, MHz range). The second term represents the viscous torque, whereas the first term on the right is the torque due to Brownian motion³⁶, with k_B the Boltzmann constant and T the absolute temperature. In both expressions, γ_r is the rotational viscosity:³²

$$\gamma_r = \frac{16\pi\eta\sqrt{a^2 - b^2}(a^4 - b^4)}{3\left(\frac{a^2 - b^2}{2}\right) \ln \frac{a + \sqrt{a^2 - b^2}}{a - \sqrt{a^2 - b^2}} - a\sqrt{a^2 - b^2}} \quad (7)$$

Here, η is the dynamic viscosity of the medium. In the case of NRs stabilized by organic ligands, a and b should be seen as the semi-axes of the NR, augmented with the length of the ligands (2 nm).

Using eq 6, we can estimate the typical time τ_{on} it takes to align an ellipsoid when switching on a sufficiently strong electric field by neglecting the Brownian term, replacing the derivative by the ratio $\Delta\theta/\tau_{on}$, and setting $\Delta\theta = \pi/4$:

$$\tau_{on} = \frac{\pi\gamma_r}{2\sqrt{2}pE + 2(\alpha_{\parallel} - \alpha_{\perp})\varepsilon_0 E^2} \quad (8)$$

$$f_{on} = \frac{1}{2\pi\tau_{on}}$$

The typical time for reorientation when switching off the voltage is called the relaxation time τ_{rel} , which is usually longer than τ_{on} . This time and the relaxation frequency can be estimated using the Debye-Perrin model and eq 6:

$$\tau_{rel} = \frac{\gamma_r}{k_B T} \quad (9)$$

$$f_{rel} = \frac{k_B T}{2\pi\gamma_r}$$

The excess electrostatic energy U_{el} of a stationary ellipsoid in an electric field is given by:

$$U_{el} = -pE \cos \theta - \frac{1}{2}[\alpha_{\perp} + (\alpha_{\parallel} - \alpha_{\perp}) \cos^2 \theta] \varepsilon_0 E^2 \quad (10)$$

In the quasi-static case, when the frequency of the field is well below f_{rel} and f_{on} , the probability $P(\theta)$ to find an ellipsoid within a given solid angle making an angle θ with the long axis of the rod is proportional to the Boltzmann distribution:

$$P(\theta) \propto \exp\left(-\frac{U_{el}}{k_B T}\right) \quad (11)$$

Light absorbance by dispersed ellipsoidal particles

When a light absorbing ellipsoidal nano-object is dispersed in a non-absorbing solvent, the effective absorption coefficient for light depends on the orientation of the particle relative to the incident electric field. Based on the depolarization factors

parallel and perpendicular to the long axis of the ellipsoid, we can write down the intrinsic absorption coefficients based on the Maxwell Garnett model³⁷

$$\mu_{\parallel} = \frac{2\pi\varepsilon_{\parallel,I}}{\lambda n_h} \left| \frac{\varepsilon_h}{\varepsilon_h + L_{\parallel}(\varepsilon_{\parallel,R} + i\varepsilon_{\parallel,I} - \varepsilon_h)} \right|^2 \quad (12)$$

$$\mu_{\perp} = \frac{2\pi\varepsilon_{\perp,I}}{\lambda n_h} \left| \frac{\varepsilon_h}{\varepsilon_h + L_{\perp}(\varepsilon_{\perp,R} + i\varepsilon_{\perp,I} - \varepsilon_h)} \right|^2$$

In this expression, n_h is the refractive index of the host solvent and $\varepsilon_{\parallel,R} + i\varepsilon_{\parallel,I}$ and $\varepsilon_{\perp,R} + i\varepsilon_{\perp,I}$ are the complex dielectric constant of the nanorod for the considered wavelength in the directions parallel and perpendicular to the NR long axis, respectively. In the typical situation for semiconductor NRs in an apolar solvent, their magnitude exceeds ε_h , resulting in a screening of the electric field by the NRs. For a prolate ellipsoid, L_{\parallel} is smaller than L_{\perp} such that the absorption coefficient for parallel orientation is the larger of the two. For an ellipsoid with inclination θ and azimuth φ as shown in Figure 3c, the absorption coefficient will be an average of μ_{\parallel} and μ_{\perp} , weighted by the square of the projection of the electric field:

$$\mu(\theta, \varphi) = \mu_{\parallel} \cos^2 \varphi \sin^2 \theta + \mu_{\perp} (1 - \cos^2 \varphi \sin^2 \theta) \quad (13)$$

For an ensemble of ellipsoids, the absorption coefficient μ in eq (13) is obtained by averaging over all orientations of the NR long axis, weighted with the corresponding Boltzmann factor (eq 11):

$$\mu = \frac{\int_0^{2\pi} \int_0^{\pi} P(\theta) \mu(\theta, \varphi) \sin \theta d\theta d\varphi}{\int_0^{2\pi} \int_0^{\pi} P(\theta) \sin \theta d\theta d\varphi} \quad (14)$$

Finally, the absorbance A of a dispersion of ellipsoidal nano-objects is given by the products of the intrinsic absorption coefficient μ and the volume fraction f of the ellipsoids and the path length d of light through the dispersion, divided by the natural logarithm of 10:

$$A = \mu \frac{fd}{\ln 10} \quad (15)$$

Results and Discussion

Full Alignment of Colloidal NRs by Electric Fields

To explore the alignment of dispersed colloidal NRs by electric fields, a dodecane-based dispersion of CdSe/CdS NRs is loaded in a cell as described in the Experimental Section. As a fraction of the NRs will carry an electric charge,³⁸ application of a DC field will make the NRs drift to the electrodes. To avoid artefacts due to NR accumulation at the electrodes, we use AC fields with a period shorter than the cell transit time $\tau_{cell} = d/uE$ where u is the mobility of the NRs. As shown in the Supporting information, NRs in a 50 μm cell have a cell transit time of ≈ 5 ms for fields of 17 V/ μm . Therefore, we use frequencies higher than 200 Hz to study NR alignment.

A first measurement involves the optical transmission of a 50 μm cell filled with a 1 μM dispersion of NRs in dodecane at

470 nm in the presence of a sinusoidal AC electric field. An example is given in Figure 4a, where it can be seen that the two extreme values of the electric field during a single period both correspond to a maximum increase of the transmission (see also the transmission of the cell in presence of a block wave electric field in Supporting Information, Figure S3). From these transmission measurements, the absorbance A by the NR dispersion is calculated as:

$$A = -\log \frac{I_T}{I_0} \quad (16)$$

Here, I_0 is the light intensity passing through the cell loaded with dodecane only, while I_T is the (possibly time dependent) intensity transmitted through the NR-loaded cell. Note that scattering by the nanorods is neglected here. One readily sees that the increased transmission upon application of an electric field corresponds to a drop of the absorbance. This is in agreement with NRs aligning their long axes parallel to the AC electric field and perpendicular to the electric field of the incident light, where the absorbance drop is due to the higher depolarization factor for fields along the short axis of the CdSe/CdS NRs ($L_{\perp} = 0.49$ instead of $L_{\parallel} = 0.018$, see Supporting Information S4, Table S1).

In order to eliminate the trivial influence of cell thickness and NR concentration from the measurements, we introduce the relative change of the absorbance $\Delta A/A_0$ (usually <0):

$$\frac{\Delta A}{A_0} = \frac{A - A_0}{A_0} \quad (17)$$

Here, A_0 is the absorbance of the NR-loaded cell in the absence of an electric field. Figure 4b represents the variation of the minimum of $\Delta A/A_0$ as a function of the applied electric field. One sees that whereas increasing the electric field initially leads to a more pronounced drop of the absorbance, $\Delta A/A_0$ levels off at ≈ -0.53 for fields exceeding $15 \text{ V}/\mu\text{m}$. This levelling-off is also apparent from the variation of $\Delta A/A_0$ over a single period of the AC field. When applying for example a 1 kHz field with a maximum amplitude of $25 \text{ V}/\mu\text{m}$, Figure 4c shows that $\Delta A/A_0$ hits a plateau each time the field is around its extreme values. The observations in Figure 4b and 4c are in good agreement with the simulated data for the alignment of nanorods with a permanent dipole moment in a homogeneous electric field. For high voltages, the theoretical model predicts that the root mean square of the inclination angle θ becomes, within a few degrees, equal to 0° or 180° . We call this full alignment. The simulations means that the average deviation angle from perfect alignment is around 9 degrees for the highest voltage applied. Figure 4c also suggests that at sufficiently high amplitudes, the NRs will be fully aligned during most of the time, except for small time intervals in which the field changes sign. Clearly, such a condition is highly beneficial if the rod orientation is to be locked in by, for example, a triggered polymerization of the surrounding medium.

Dynamical Properties of Colloidal NR Alignment

Next to the levelling off of the absorbance change, Figure 4c also makes clear that the change in absorbance is established without noticeable delay. This indicates that at the fields and frequencies used, the NRs readily flip from a $\theta = 0^\circ$ to a $\theta = 180^\circ$ orientation when the field changes direction (see Figure 3c for a definition of the angle θ).

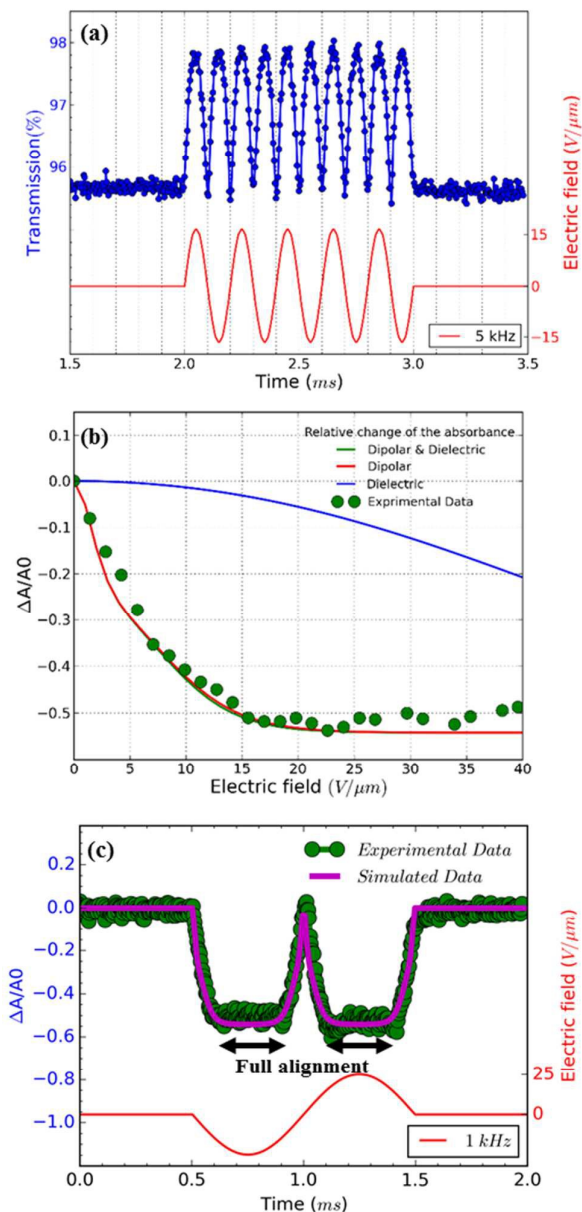


Figure 4 (a) Transmission measurements (blue dots) of a CdSe/CdS NR suspension for blue light ($\sim 470 \text{ nm}$) with and without the presence of a sinusoidal AC electric field with a frequency of 5 kHz and an amplitude of $17 \text{ V}/\mu\text{m}$ (red line). (b) Minimum value of the relative change of the absorbance of the $1 \mu\text{Molar}$ NR dispersion in the presence of an AC electric field with a frequency of 1 kHz as a function of peak value of the electric field. Measurements (green dots) and simulations assuming only dielectric torque (blue), only dipolar torque (red) and both dielectric and dipolar torques (green, almost identical to red). (c) Relative change of the measured (green dots) and simulated (magenta) absorbance of the $1 \mu\text{Molar}$ NR dispersion for blue ($\sim 470 \text{ nm}$) light in the presence of an AC electric field with frequency 1 kHz and amplitude $25 \text{ V}/\mu\text{m}$ (red).

Hence, the NR reorientation occurs on a time scale much shorter than the 1 ms period of the AC field, an outcome in line with the dynamical properties of NR (re)orientation. Indeed, using eqs 7 and 9, the rotational relaxation frequency f_{rel} in dodecane of the CdSe/CdS NRs used here can be estimated at 13 kHz (see Supporting Information S4, Table S1).

Hence, fields with a frequency well below 13 kHz, should give the NRs enough time to establish a quasi-equilibrium Boltzmann distribution that follows the variation of the electric field, thus bringing them from random orientation to full alignment. In line with this, increasing the AC frequency from 1 to 10 kHz only changes the frequency at which the transmission changes, without affecting the limiting value corresponding to full alignment (see Supporting Information S5). Hence, the only difference between a 1 and a 10 kHz field is that the latter makes the NRs flip faster between the $\theta = 0^\circ$ to a $\theta = 180^\circ$ orientation.

At frequencies above f_{rel} , we expect that the distribution will not return to random alignment and the minimum in the transmission will not be as low as the zero-field transmission. Moreover, the NRs will stop reacting to the AC field once the frequency exceeds the turn on frequency f_{on} , which is estimated at ≈ 100 kHz in this case (see Supporting Information S4, Table S1). This description of the NR orientation dynamics is further confirmed by the response of the transmission to a single block pulse with an amplitude of $17 \text{ V}/\mu\text{m}$. As shown in Figure 5, the regimes of full alignment and de-alignment are reached within less than $50 \mu\text{s}$.

Permanent versus Induced Dipole Moments

As the absorbance of the CdSe/CdS NRs at 470 nm will be dominated by the CdS rod (Figure 1b), the bulk optical constants of CdS can be used to estimate the dielectric function of the nanorod in the expressions for the polarizability and the absorption coefficient of dielectric ellipsoids, i.e., eq 2 and 14, respectively. The thus calculated polarizability and absorption coefficients at 470 nm have been summarized in Supporting Information S4, Table S1. Using these figures, the degree of orientation and the concomitant relative absorbance change can be calculated if only the dielectric torque were present. The thus predicted dependence of $\Delta A/A_0$ on the electric field strength has been added to Figure 4b, where it follows that fields of more than $40 \text{ V}/\mu\text{m}$ would be needed to obtain an appreciable alignment of the NRs. We therefore conclude that the (full) alignment of the NRs is indeed due to the permanent dipole moment of the NRs. Considering the NR dipole moment p as an adjustable parameter, the field dependence of $\Delta A/A_0$ can again be predicted. Figure 4b shows that taking $p = 1500 \text{ D}$, a typical value for the CdSe/CdS NRs used here, makes the simulated field dependency of $\Delta A/A_0$ closely match the experimental data. We stress that this predicted trend depends on a single adjustable parameter, i.e., the dipole moment p , which mainly determines the region of electric fields where the NRs change from random to full alignment. The high-field limit of $\Delta A/A_0$ on the other hand only depends

on the difference in absorption coefficient of fully aligned (μ_{\perp}) and randomly aligned (μ_0) quantum rods:

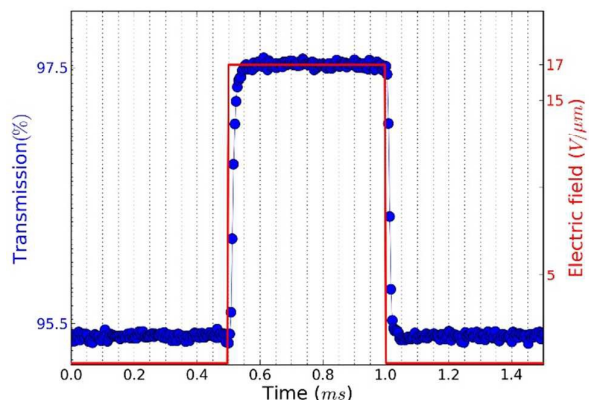


Figure 5 Transmission versus time of a CdSe/CdS NR suspension in dodecane when a pulse with amplitude of $17 \text{ V}/\mu\text{m}$ is applied.

$$\lim_{E \rightarrow \infty} \frac{\Delta A}{A_0} = \frac{\mu_{\perp} - \mu_0}{\mu_0} \quad (18)$$

Inserting the estimated absorption coefficients (see Supporting Information, Table 1), a limit of -0.54 is obtained, in line with the experimental findings.

Absorption Anisotropy at the Band-Edge Transition

As indicated by eq 18, the regime of full alignment provides a way to directly determine the absorption anisotropy of colloidal NRs at any given wavelength. We therefore extended the analysis to the NR absorbance at the CdSe/CdS first exciton transition at around 560 nm (see Figure 1b), which is due to electronic transitions between quantized states in the CdSe core. To adjust for the absorbance difference at 470 and 560 nm of the CdSe/CdS NRs, we had to analyze NR dispersions with a concentration 10 times higher than used for the previous measurements. Hence, we now measure the transmission of green light ($\approx 560 \text{ nm}$) through a $50 \mu\text{m}$ thick cell filled with a $10 \mu\text{M}$ NR dispersions in the presence of an AC electric field ($17 \text{ V}/\mu\text{m}$, 1 kHz). Figure 6a shows that the AC field leads to a similarly oscillating increased transmission – meaning a decrease in absorbance – as observed before at 470 nm. Hence, also the CdSe core transitions exhibit a marked absorption anisotropy. An issue with the more concentrated dispersions used here is that a considerable fraction of the NRs form aggregates that are not oriented by the applied electric field. Figure 6b therefore compares the relative change of the absorbance determined at 560 nm with that determined at 470 nm for the same dispersion under the same conditions of the applied field. Since this transmission change would reach -0.54 if all rods aligned, the actual plateau value can be used to estimate the fraction of NRs that can be aligned and thus calibrate the transmission changes at 560 nm.

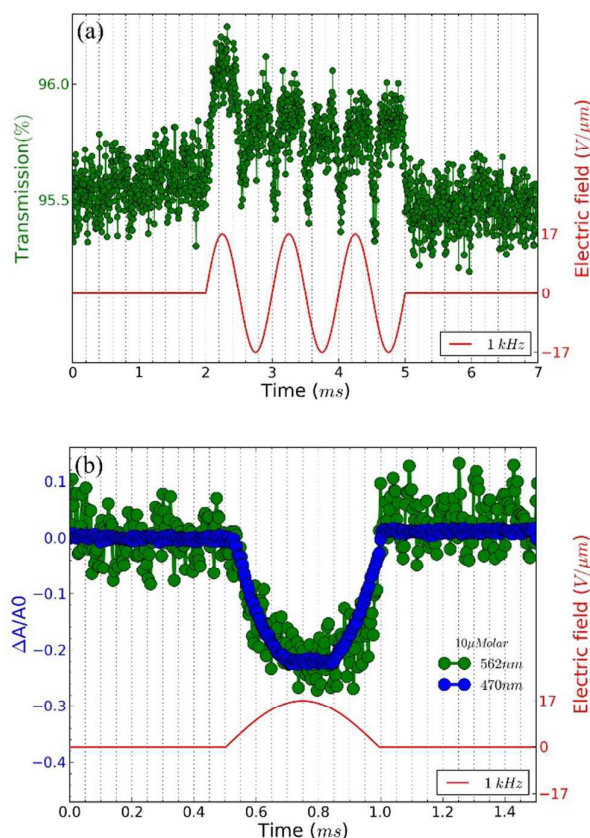


Figure 6. (a) Transmission measurement (green dots) of a NR suspension for green (~560 nm) light in the presence of an AC electric field with frequency 1 kHz and amplitude 17 V/μm (red) (b) Relative change of the measured absorbance of the 10 μMolar NR dispersion for blue light (blue dots) and green light (green dots) in the presence of an AC electric field with frequency 1 kHz and amplitude 17 V/μm (red).

Figure 6b shows that this calibration is actually quite straightforward since the high-field limit of $\Delta A/A_0$ (eq.17) at 560 nm due to CdSe core absorption is very similar to the one measured at 470 nm, which is due to absorption in the CdS rod. Hence, a quite similar corrected limiting value of $\Delta A/A_0$ in the range -0.5 to -0.55 is obtained at the band-gap transition as well. This result may seem surprising since the core is a spherically symmetric object, yet it can be understood by realizing that the dielectric mismatch between the CdSe core and the CdS shell is small.

To clarify this point, Figure 7 shows the electric field distribution within a CdS ellipsoid encompassing a CdSe sphere and surrounded by dodecane as a host. This field has been obtained from a 3D finite element field calculation modelling all materials by means of the real parts of the anisotropic bulk dielectric functions at 560 nm (see Supporting Information S4, Table S2). Regardless of the orientation of the NR relative to the external field, we find that the internal field in the CdSe core amounts to $\approx 95\%$ of the field in the CdS host.

Moreover, the electric field in the rod (and thus the sphere) is

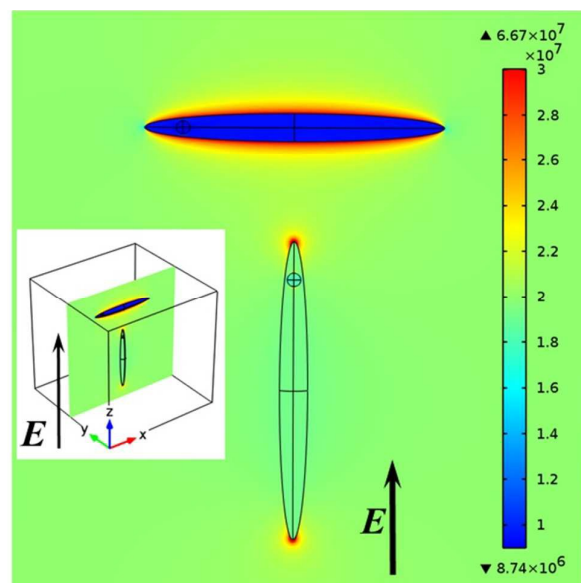


Figure 7. Simulation of the field distribution (V/m) inside a dot in rod using the bulk dielectric function for incident light parallel and perpendicular to the c-axis of the rod at 560 nm. The minimum and maximum values of the field are indicated next to the triangles. (Inset: 3D structure shows the position of the NRs in the medium).

almost identical to the external electric field when the applied field is parallel to the c-axis of the rod, while it is only about half the applied external field for the perpendicular orientation.

These internal fields closely agree with the internal fields in CdS-only ellipsoids with depolarization factors $L_{\parallel} = 0.018$ and $L_{\perp} = 0.49$ dispersed in dodecane. The CdSe core thus experiences the same enhanced or reduced screening of the internal field as the CdS rod for incident optical fields perpendicular to or parallel with the long axis of the NR. Hence the largely similar absorption anisotropy for the quantum-dot band gap transition.

Note that the experimentally determined high-field limit of $\Delta A/A_0$ corresponds to a polarization ratio of 64% for the emission (see Supporting Information, S6), which is similar to the experimentally determined values of up to 75% as determined on single CdSe/CdS NRs.⁵

Conditions to reach full alignment

According to formula (11), full alignment is obtained when the difference in electrostatic energy U_{el} between parallel and perpendicular alignment is considerably larger than kT . Because we found that the contribution from the induced dipole moment is relatively small, the difference in electrostatic energy is in good approximation given by $-E \cdot p$ according to equation (10). Based on the experimental result that a dipole moment of 1500 D requires a threshold field E_{th} of 17 V/μm, we can estimate the field necessary to align dipoles with a different dipole moment p by:

$$E_{th} \approx 20 \frac{k_B T}{p} \quad (19)$$

Conclusions

We have shown that colloidal CdSe/CdS NRs can be fully aligned in a colloidal dispersion by the application of AC electric fields with an appropriate field strength. The alignment is monitored by measuring the variation of the transmission concurring with the oscillation of the electric field at wavelengths where the CdS rod absorption dominates. For the rods used, complete alignment parallel with the electric field is obtained for field strengths exceeding $15 \text{ V}/\mu\text{m}$ and switching back and forth to random orientation occurs within $50 \mu\text{s}$. We develop a theoretical description of the relation between the electric field and the alignment of dielectric ellipsoidal nano-objects, considering both a permanent and an induced dipole moment. Doing so, it follows that the experimentally determined alignment as a function of field strength can be attributed to the interaction between the NR permanent dipole and the applied AC field.

Since the transmission change in the regime of full alignment only depends on the difference between the NR absorption coefficient for optical fields parallel and perpendicular to the NR long axis, transmission measurements during AC driven full alignment provide an excellent method to measure anisotropic absorption by NRs. Excellent agreement between experiment and theory is obtained for the absorption anisotropy at 470 nm , i.e., wavelengths where the rod absorption dominates. Moreover, we find that band-edge transition exhibits a quite similar absorption anisotropy, a result we attribute to the small dielectric mismatch between the CdSe core and the CdS rod.

Acknowledgements

This research was supported by the Interuniversity Attraction Poles program of the Belgian Science Policy Office, under grant IAP P7-35.

References

1. E. R. Smith, J. M. Luther and J. C. Johnson, *Nano letters*, 2011, **11**, 4923-4931.
2. J. Cao, T. Sun and K. T. V. Grattan, *Sensors and Actuators B-Chemical*, 2014, **195**, 332-351.
3. M. Shim and H. McDaniel, *Current Opinion in Solid State & Materials Science*, 2010, **14**, 83-94.
4. Z. Hens and I. Moreels, *Journal of Materials Chemistry*, 2012, **22**, 10406-10415.
5. F. Pisanello, L. Martiradonna, P. Spinicelli, A. Fiore, J. P. Hermier, L. Manna, R. Cingolani, E. Giacobino, A. Bramati, M. De Vittorio and I. Ieee, *Polarized Single Photon Emission for Quantum Cryptography Based on Colloidal Nanocrystals*, Ieee, New York, 2009.
6. R. Krahne, G. Morello, A. Figuerola, C. George, S. Deka and L. Manna, *Physics Reports-Review Section of Physics Letters*, 2011, **501**, 75-221.
7. K. Becker, J. M. Lupton, J. Muller, A. L. Rogach, D. V. Talapin, H. Weller and J. Feldmann, *Nature Materials*, 2006, **5**, 777-781.
8. W. S. Chang, J. W. Ha, L. S. Slaughter and S. Link, *Proceedings of the National Academy of Sciences of the United States of America*, 2010, **107**, 2781-2786.
9. A. Rizzo, C. Nobile, M. Mazzeo, M. De Giorgi, A. Fiore, L. Carbone, R. Cingolani, L. Manna and G. Gigli, *Acs Nano*, 2009, **3**, 1506-1512.
10. M. Fisher, M. Zanella, D. J. Farrell, L. Manna, P. Stavrinou and A. J. Chatten, *2011 37th IEEE Photovoltaic Specialists Conference (PVSC 2011)*, 2011, 000858-000863000863.
11. C. Nobile, V. A. Fonoberov, S. Kudera, A. Della Torre, A. Ruffino, G. Chilla, T. Kipp, D. Heitmann, L. Manna, R. Cingolani, A. A. Balandin and R. Krahne, *Nano letters*, 2007, **7**, 476-479.
12. F. Liu, J. Wang, Z. Ge, K. Li, H. Ding, B. Zhang, D. Wang and H. Yang, *Journal of Materials Chemistry C*, 2013, **1**, 216-219.
13. A. Persano, M. De Giorgi, A. Fiore, R. Cingolani, L. Manna, A. Cola and R. Krahne, *Acs Nano*, 2010, **4**, 1646-1652.
14. A. Singh, R. D. Gunning, S. Ahmed, C. A. Barrett, N. J. English, J. A. Garate and K. M. Ryan, *Journal of MateriChemistry*, 2012, **22**, 1562-1569.
15. C. Querner, M. D. Fischbein, P. A. Heiney and M. Drndic, *Adv. Mater.*, 2008, **20**, 2308.
16. A. Ghezelbash, B. Koo and B. A. Korgel, *Nano Letters*, 2006, **6**, 1832-1836.
17. D. V. Talapin, E. V. Shevchenko, C. B. Murray, A. Kornowski, S. Forster and H. Weller, *Journal of the American Chemical Society*, 2004, **126**, 12984-12988.
18. M. Zanella, R. Gomes, M. Povia, C. Giannini, Y. Zhang, A. Riskin, M. Van Bael, Z. Hens and L. Manna, *Advanced Materials*, 2011, **23**, 2205.
19. J. L. Baker, A. Widmer-Cooper, M. F. Toney, P. L. Geissler and A. P. Alivisatos, *Nano Letters*, 2010, **10**, 195-201.
20. Y. Amit, A. Faust, I. Lieberman, L. Yedidya and U. Banin, *Physica Status Solidi a-Applications and Materials Science*, 2012, **209**, 235-242.
21. Z. H. Hu, M. D. Fischbein, C. Querner and M. Drndic, *Nano letters*, 2006, **6**, 2585-2591.
22. K. M. Ryan, A. Mastroianni, K. A. Stancil, H. T. Liu and A. P. Alivisatos, *Nano Letters*, 2006, **6**, 1479-1482.
23. M. Mohammadimasoudi, L. Penninck, T. Aubert, R. Gomes, Z. Hens, F. Strubbe and K. Neyts, *Opt Mater Express*, 2013, **3**, 2045-2054.
24. A. Singh, N. J. English and K. M. Ryan, *Journal of Physical Chemistry B*, 2013, **117**, 1608-1615.
25. D. Baranov, A. Fiore, M. van Huis, C. Giannini, A. Falqui, U. Lafont, H. Zandbergen, M. Zanella, R. Cingolani and L. Manna, *Nano Letters*, 2010, **10**, 743-749.
26. N. Zhao, K. Liu, J. Greener, Z. H. Nie and E. Kumacheva, *Nano Letters*, 2009, **9**, 3077-3081.
27. A. M. Hung, N. A. Konopliv and J. N. Cha, *Langmuir*, 2011, **27**, 12322-12328.
28. A. M. Hung, T. Oh and J. N. Cha, *Nanoscale*, 2012, **4**, 1016-1020.
29. F. Pietra, F. T. Rabouw, P. G. van Rhee, J. van Rijssel, A. V. Petukhov, B. H. Ern , P. C. M. Christianen, C. de Mello Doneg  and D. Vanmaekelbergh, *Acs Nano*, 2014, **8**, 10486-10495.
30. L. S. Li and A. P. Alivisatos, *Physical Review Letters*, 2003, **90**, 097402.

Journal Name

ARTICLE

31. J. S. Kamal, R. Gomes, Z. Hens, M. Karvar, K. Neyts, S. Compennolle and F. Vanhaecke, *Physical Review B*, 2012, **85**, 035126.
32. H. E. Ruda and A. Shik, *Nanotechnology*, 2010, **21**, 235502
33. R. Krishnan, M. A. Hahn, Z. H. Yu, J. Silcox, P. M. Fauchet and T. D. Krauss, *Phys. Rev. Lett.*, 2004, **92**, 216803
34. L. D. Landau, Lifshitz, Evgenii Mikhailovich, *Electrodynamics of continuous media* Oxford 1984, 331.
35. A. Sihvola, *Journal of Nanomaterials*, 2007.
36. G. Volpe and D. Petrov, *Phys. Rev. Lett.*, 2006, **97**, 210603.
37. D. Ricard, M. Ghanassi and M. C. Schanneklein, *Optics Communications*, 1994, **108**, 311-318.
38. M. Cirillo, F. Strubbe, K. Neyts and Z. Hens, *Acs Nano*, 2011, **5**, 1345-1352.